J. Webster (ed.), *Wiley Encyclopedia of Electrical and Electronics Engineering*

PYROELECTRICITY

Some crystalline materials exhibit intrinsic polar behavior due to the atomic arrangements in the unit cells of their crystalline structure. In these structures, charge dipoles occur or sometimes the centers of the positive and negative charges do not coincide or overlap each other in specific directions. As a result a net dipolar moment exists in the material which is equal to the charge multiplied by the charge separation of the positive and negative centers (Fig. 1). The total dipole moment per unit volume depends on the chemistry of the material and the atomic arrangement in a particular material's crystallographic structure. The total dipole moment per unit volume is defined as polarization P, in a material.

Obviously if the temperature of the material changes, the separation of the ionic charges or dipole moment or polarization varies in the crystal. The voltage or current resulting from the change in polarization or dipole moment caused by the variation in temperature is the pyroelectric effect, and the phenomenon is pyroelectricity. The word "pyro" derived from Greek means heat.

If a piece of tourmaline (one of the minerals in which this property was first identified) is held at a constant temperature, charge separation does not vary, and the crystal is electrically neutral. If, for example, we pick up and hold a tourmaline crystal (body temperature $\sim 37^{\circ}$C) which is at room temperature $\sim 20^{\circ}$C, the electrical polarization of the material changes and hence a voltage is developed between the faces perpendicular to the polar axis. The magnitude of the voltage generated could be several kilovolts per centimeter. Conversely, if the temperature of the material drops from 37° to 20°C, the same voltage magnitude of opposite polarity is generated.

As a result, these materials are used as thermal sensors in applications such as burglar alarms, medical diagnostic instruments, fire alarms, night vision devices or infrared (thermal radiation) TV, and laser power meters. Pyroelectric materials detect temperature variations as small as one millionth of a degree. In most thermal sensing devices, the pyroelectric material element works as a thermal transducer, as shown in Fig. 2.

The pyroelectric coefficient p of a material under constant stress and electric field is defined by the expression

$$p = \left(\frac{\partial P}{\partial T}\right)_{E,\sigma} \qquad (1)$$

where P is the polarization, T the temperature, E the electric field, and σ the elastic stress.

The pyroelectric effect occurs only in those materials whose point group symmetry is consistent with the vectorial property of the polarization. Thus crystalline materials whose structures belong to the ten polar point groups, namely, 1, m, 2, mm2, 3, 3m, 4, 4mm, 6, 6mm, and ceramics, polymeric, and composite materials whose structures belong to the textural or Curie point groups (∞, ∞m) are pyroelectric materials. Thus the pyroelectrics can be classified into two main categories: (1) nonferroelectric pyroelectrics, those whose polarization cannot be switched by applying an external electric field (including some semiconductors and biological materials) and (2) ferroelectric pyroelectrics whose polarization is obtained by poling and also is switched by an electric field.

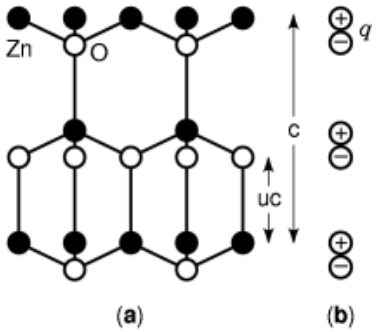

Fig. 1. In the atomic arrangement of the hexagonal structure (wurtzite) of zinc oxide (ZnO), Zn-O dipoles are present along the crystallographic polar c-axis of the crystal. The c-lattice constant is defined for a crystal terminated in the configuration shown in (b). The dipole moment can be estimated here as charge (q) $\times$ (c/2-uc), where u is a positional parameter typically equal to 3/8 for such atomic arrangements.

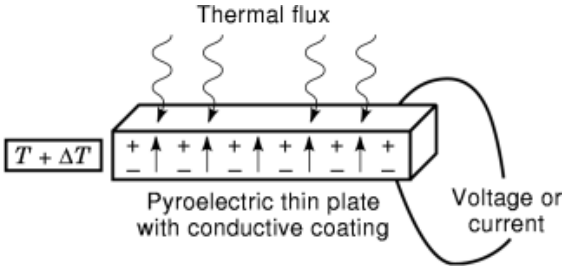

Fig. 2. A thin plate of pyroelectric material is first coated on both sides, perpendicular to the dipole direction, with the conductive thin films or electrode materials (arrow indicates the ionic dipole). When this plate is submerged in or exposed to a variable thermal flux causing its temperature T to change by ΔT, a voltage or current is generated which is related to the rate and magnitude of the temperature change.

The pyroelectric effect of ferroelectric pyroelectrics usually exists below a certain transition temperature called the Curie point Tc in the proper ferroelectrics and is more temperature-dependent than that of the nonferroelectric pyroelectrics.

Thermodynamic analysis of the pyroelectric effect yields the expression

$$p_i^{\sigma} = p_i^{\epsilon} + d_{ijk}^{T} c_{jklm}^{T,E} \alpha_{lm}^{\sigma} \qquad (2)$$

where $p^{\sigma}{}_i$ is the total pyroelectric effect measured at constant stress, and $p^{\varepsilon}{}_i$, the pyroelectric effect at constant strain ε, is called the primary effect. The second term of Eq. (2), the contribution caused by thermal deformation of the crystal, is known as the secondary pyroelectric effect. The piezoelectric, elastic stiffness, and thermal expansion coefficients of the crystal are d, c, and α, respectively. (A third contribution to the pyroelectric effect, known as the tertiary pyroelectric effect, arises from inhomogeneous temperature distributions within the sample. Because the tertiary effect depends on experimental conditions, it is not included in this article.)

In ferroelectric pyroelectrics the primary effect generally is large and negative because spontaneous polarization diminishes with increasing temperature. The secondary effect is considerably smaller and may have either sign depending on the values of the constants. Thus experimentally observed pyroelectric coefficients are dominated by the primary effect and are negative in ferroelectric crystals. In nonferroelectric pyroelectric

crystals there is no simple way to predict the sign and the magnitude of these coefficients. In practice the total pyroelectric effect is measured and the secondary effect is calculated from the constants d, α, and c.

For a number of applications, such as infrared detectors and vidicons, it is desirable to know the magnitude and sign of the contributions to the total pyroelectric effect. The secondary contributions for various crystal symmetry groups can be calculated from the following equations:

$$\begin{aligned} p_{\text{sec}} = {} & d_{21}(c_{11}\alpha_1 + c_{12}\alpha_2 + c_{13}\alpha_3 + c_{15}\alpha_5) \\ & + d_{22}(c_{12}\alpha_1 + c_{22}\alpha_2 + c_{23}\alpha_3 + c_{25}\alpha_5) \\ & + d_{23}(c_{13}\alpha_1 + c_{23}\alpha_2 + c_{33}\alpha_3 + c_{35}\alpha_5) \\ & + d_{25}(c_{15}\alpha_1 + c_{25}\alpha_2 + c_{35}\alpha_3 + c_{55}\alpha_5) \end{aligned} \tag{3}$$

for point group 2 and b as polar axis;

$$\begin{aligned} p_{\text{sec}} = {} & d_{31}(c_{11}\alpha_1 + c_{12}\alpha_2 + c_{13}\alpha_3) \\ & + d_{32}(c_{12}\alpha_1 + c_{22}\alpha_2 + c_{23}\alpha_3) \\ & + d_{33}(c_{13}\alpha_1 + c_{23}\alpha_2 + c_{33}\alpha_3) \end{aligned} \tag{4}$$

for point group mm2 and c as polar axis; and

$$\begin{aligned} p_{\text{sec}} = {} & 2d_{31}(c_{11}\alpha_1 + c_{12}\alpha_1 + c_{13}\alpha_3) \\ & + d_{33}(2c_{13}\alpha_1 + c_{33}\alpha_3) \end{aligned} \tag{5}$$

for point groups 3, 3m, 4, 4mm, 6, 6mm, and c as polar axis.

Point group ∞m of the poled ceramic sample leads to equations equivalent in form to the hexagonal crystal system. The ∞ axis is parallel to the poling direction and is denoted as x_3. The primary and secondary pyroelectric components of a few materials are listed in Table 1.

The values of the constants are taken from the literature and from the Landolt–Börnstein Tables on physical constants of materials. It is evident from the data that both the primary and total pyroelectric effects in ferroelectric ceramics and single crystals are large and negative. Secondary coefficients in ferroelectric single crystals are comparatively small and positive with the exception of SBN and $NaNO_2$ whose secondary pyroelectric effect is small and negative, enhancing the primary pyroelectric effect. The secondary effect is substantial in triglycine sulphate (*TGS*), $Ba_2NaNb_5O_{15}$, and the ceramics $Pb(ZrTi)O_3$ and $BaTiO_3$.

Compared to ferroelectrics, tourmaline and other nonferroelectric polar materials have rather small pyroelectric effects. The total and the secondary coefficients of these materials carry the same sign, and in most cases they are positive. The secondary effect arising from piezoelectricity and thermal expansion is a large contributor to the total pyroelectric effect. In tourmaline, for instance, 80% of the pyroelective effect is of secondary origin. Fresnoite, $Ba_2TiSi_2O_8$, is another mineral in which pyroelectricity is dominated by the secondary effect. In semiconductor pyroelectrics that have the wurtzite structure, the effect is very small, and all coefficients have the same sign.

It is clear from the Table 1 that both the primary and secondary effects are important, and certain trends emerge in the magnitude and sign of the coefficients. All pyroelectric materials do not follow the same pattern, but members of the same family share common features. In ferroelectrics all of the coefficients are negative and dominated by the primary effect, in contrast to non-ferroelectric pyroelectrics where secondary effects can be more substantial.

Table 1. Primary, Secondary, and Observed Pyroelectric Effects in Various Pyroelectric Materials[a]

Materials	Point Group Symmetry	Observed Total Effect $\mu C/(m^2 \cdot K)$	Calculated Secondary Effect $\mu C/(m^2 \cdot K)$	Primary Effect $\mu C/(m^2 \cdot K)$
Ferroelectrics				
Ceramics				
				−110.0
		−50	+60	−270.0
$Pb(Zr_{0.52}Ti_{0.48})O_3$: 1 wt% Nb_2O_5 (PZT)	∞mm	−190.0	+80.0	−305.7
$BaTiO_3$	∞mm	−268.0	+37.7	
$Pb(Zr_{0.95}Ti_{0.05})O_3$: 1 wt% Nb_2O_5 (PZT)	∞mm			−529.0
Single crystal		−550	−21.0	−330.0
$Sr_{0.5}Ba_{0.5}Nb_2O_6$ (SBN)	4mm	−270	+60.0	−178
$(NH_2CH_2COOH)_3 \cdot H_2SO_4$ (TGS)[b]	2	−176	+2.00	−95.9
$LiTaO_3$	3m	−83.0	+12.9	−110.5
$LiNbO_3$	3m	−95.0	+15.5	−141.8
$Pb_5Ge_3O_{11}$	$\bar{3}$	−100.0	+41.8	−135.0
$Ba_2NaNb_5O_{15}$[c]	2mm	−140.0	−5.0	
$NaNO_2$	2mm			+60.2
Nonferroelectrics		+86.3	+26.1	+0.8
$Li_2SO_4 \cdot H_2O$	2	+4.0	+3.2	−92.0 ×
Tourmaline	3m	+25 ×	+117 ×	10^{-4}
Bone	∞	10^{-4}	10^{-4}	−12.0,
$Ba_2Si_2TiO_8$ (Fresnoite)	4mm	+10	+22, +16	−6.0
Li_2GeO_3	2mm	−27	−12.8	−14.2
$Ba(NO_3)_2 \cdot H_2O$		−25.3	−3.3	−22.0
Semiconductors (wurtzite structure)				
CdS	6mm	−4	−1.0	−3.0
CdSe	6mm	−3.5	−0.56	−2.94
ZnO	6mm	−9.4	−2.5	−6.9
ZnS[d]	6mm	0.43	+0.34	
BeO	6mm	−3.40	−0.008	−3.39

[a] Room temperature values.
[b] Average value of the wide range of reported values between 200 to 350 $\mu C/(m^2 \cdot K)$.
[c] Maximum value of p measured on the sample.
[d] No reported sign for p^c; no information about polytypic nature of the sample.

Pyroelectric materials are used in a wide range of applications in everyday life and in highly technologically oriented fields.

For the convenience of application engineers, simple expressions to aid in the material selection for a specific device and several figures of merit criteria are defined. Most of those can be calculated from the thermal, electrical, and optical characteristics of the materials available in the literature and various handbooks on the

physical constants of materials. The following are the four major figures of merit:

1. $F_{\mathrm{D}} = \dfrac{p}{C_p \rho \sqrt{\epsilon_0 \kappa \tan\delta}}$ pyroelectric point detector
2. $F_i = \dfrac{p}{C_{\mathrm{p}} \rho}$ fast pulse detector
3. $F_{\mathrm{V}} = \dfrac{p}{C_{\mathrm{p}} \rho \epsilon_0 \kappa}$ large area detector
4. $F_{\mathrm{Vid}} = \dfrac{p\gamma}{C_p \rho \epsilon_0 \kappa}$ vidicon

where C_{P} is the specific heat, ρ is the density, ε_0 is the vacuum permittivity (8.85×10^{-12} F/m), κ is the dielectric constant, $\tan\delta$ is the dielectric loss tangent, γ is the reciprocal thermal diffusivity and p is the pyroelectric coefficient of the material at the operating temperature of the device.

Although expression (1) evaluates the material characteristics for the point detector, the figure of merit (2) is sufficient to select suitable material for fast high-power laser pulse detectors. Expression (3) is good for large area detectors. For infrared imaging systems where array designs are desirable, expression (4) for the figure of merit, which includes thermal diffusivity, is suitable.

In several pyroelectric device designs an induced pyroelectric effect (caused by the electric field) has been exploited. The induced pyroelectric coefficient p_{ind} is defined as

$$p_{\mathrm{ind}} = \epsilon_0 E \frac{d\kappa}{dT} \tag{6}$$

where E is the applied field and T is the temperature. The sign of the p_{ind} is defined by the electric field vector. The material figure of merit for this category is expressed as

$$\frac{p_{\mathrm{ind}}\gamma}{C_{\mathrm{p}} \rho \sqrt{\kappa(E) \tan\delta(E)}} \tag{7}$$

where $\kappa(E)$ and $\tan\delta(E)$ are the dielectric constant and the dielectric loss factor, respectively, of a material in a specific electric field.

Materials of interest in this category are usually high dielectric constant relaxors and ferroelectric crystals and ceramics with a dispersive nature and a Curie point near room temperature. These materials are important for large area infrared imagers.

It is clear from the previous expressions that high p/κ is the first clue in selecting a material suitable for pyroelectric devices.

The materials most suitable for pyroelectric devices are listed in Tables 2 and 3.

Several modified TGS compositions have attractive pyroelectric properties (Table 3) and thus are useful for highly sensitive IR imagers. In Table 3 various materials represented by letters have been used to dope or modify TGS.

Figure 3 shows the typical p, κ, and p/κ, and their temperature dependencies for a single crystal of ATGSAs.

In proper ferroelectrics, a simple phenomenological approach is suggested to relate the pyroelectric figure of merit p/κ to more basic parameters of the pyroelectric crystals (Bhalla et al. and Liu et al.). For a very wide family of displacive and order-disorder ferroelectrics, an empirical relationship $= 3 \times 10^{-9}$ C·cm^{-2}·deg.$^{-1}$

Table 2. Pyroelectric Properties of Important Pyroelectrics at 25°C

Material	p, $\mu C/m^2 \cdot K$	Dielectric Properties κ	Dielectric Properties $\tan\delta$	C'_p,[g] 10^6 $Jm^{-3}K^{-1}$	K,[f] 10^{-7} m^2S^{-1}	T_C, °C	F_V, m^2C^{-1}	F_D, $10^{-5}Pa^{-1/2}$	F_{vid}, $10^6 nC^{-1}$
PVDF	270	12 (10 Hz)	0.015 (10 Hz)	2.43	0.62	80+	0.1	0.88	1.6
LiTaO3	230	47	10^{-4} to 5×10^{-3}	3.2	13.0	665	0.17	35.2 to 4.9	0.13
SBN50[a]	550	400	3×10^{-3}	2.34		121	0.07	7.2	
PZFNTU[b] Ceramics	380	290 (1 kHz)	2.7×10^{-3} (1 kHz)	2.5		230	0.06	5.8	
PCWT[c] 4/24 Ceramics	380	220 (1.5 kHz)	0.011 (1.5 kHz)	2.5		255	0.08	3.3	
[4]PGO[d]	110	40	5×10^{-4} (100 Hz)	2.0	3.0	178	0.16	13.1	0.5
[5]PGO : Ba3[e]	320	81	1×10^{-3} (100 Hz)	2.0	3.0	70	0.22	8.4	0.7
TGS	550 (35°C)	55	0.025	2.6	3.3	49	0.43	6.1	1.3
DTGS	550 (40°C)	43	0.020	2.4	3.3	61	0.60	8.3	1.8
TGFB	700 (60°C)	50	0.028	2.6	3.3+	73	0.61	7.6	1.8
ATGSAs	700	32	<0.010			51	0.99*	>16.6*	3.0

[a] SBN50: $Sr_{0.5}Ba_{0.5}Nb_2O_6$.
[b] PZFNTU: $PbZrO_3$: $PbTiO_3$: $PbFe_{0.5}Nb_{0.5}O_3$.
[c] PCWT4/24: $(Pb_{0.76}Ca_{0.24})(Co_{0.5}W_{0.5})_{0.04}Ti_{0.96}O_3$.
[d] PGO: $Pb_5Ge_3O_{11}$.
[e] PGO: Ba3 : $Pb_{4.7}Ba_{0.3}Ge_3O_{11}$.
[f] Thermal conductivity.
[g] $C'_p = \rho C_P$.

Table 3. Pyroelectric Properties of the TGS Family[a]

Material[b]	κ	p, $\mu C/m^2 \cdot K$	P_s, $\mu C/cm^2$	T_c, °C	p/κ, $10\ \mu C/m^2 \cdot K$
TGS	30	330	3.0	49	1.1
DTGS	19	270		62	1.4
TGFB	14–16	210–140		73	1.5
DTGFB	11–14	190–240	4.3	75	1.7
LTGS	40	400	3.7	49	1.0
MTGS	40	560	4.6	49	1.2
ATGSP (25°C)	30–32	650	5.0	51	2.0
ATGSAs (25°C)	32	700	6.0	51	2.1–2.3
ADTGSP	22	460	5.3	60	2.1
ADTGSAs	23	500	6.2	62	2.2

[a] Optimum temperature.
[b] D = deuterium; B = beryllium; F = fluorine; M = manganese; P = phosphorous; As = arsenic; L = lithium; and A = alanine.

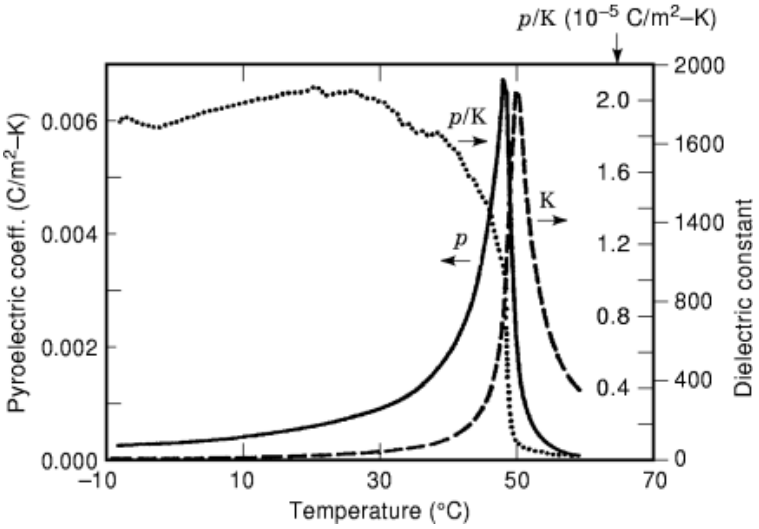

Fig. 3. Temperature dependence of p, κ, and p/κ for ATGSAs (alanine- and arsenic-doped triglycine sulphate) crystal.

applies, whereas for several modified triglycine sulfate (TGS) crystals, the relationship $p/\kappa^{3/4} = 3 \times 10^{-9}$ C·cm^{-2}·deg.$^{-1}$ holds nicely. Figure 4 summarizes the results for most ferroelectric pyroelectrics.

Methods for Determining Pyroelectric Coefficients

There are several methods for measuring pyroelectric coefficients, but most of those can be grouped into two categories. The objective in the first category is to measure the pyroelectric current directly and at the same time vary the temperature. The temperature variation can be generated by using the chopping incoming radiation source or ac heating (known as the Chynoweth technique) of the sample. The pyroelectric response current i is expressed as

$$i = \frac{p\eta W T_r}{C' t} \tag{8}$$

where ηW is the power absorbed by the sample, T_r is a transfer function depending on the thermal circuit of the sample and the chopping or modulation frequency, t is the thickness of the sample, and C' is the thermal capacity of the sample. Often a thin layer of highly absorbing material is applied on the sample surfaces to achieve $\eta = 1$. The pyroelectric current $i(T)$ at a temperature T, can also be measured by uniformly heating or cooling the sample at a constant rate (in general 1 to 4°C/min) and the pyroelectric coefficient p is calculated from the following expression (Byer–Roundy technique):

$$i(T) = \frac{Ap}{\Delta T/\Delta t} \tag{9}$$

where A is the electroded area of the sample and $\Delta T/\Delta t$ is the heating or cooling rate of the sample.

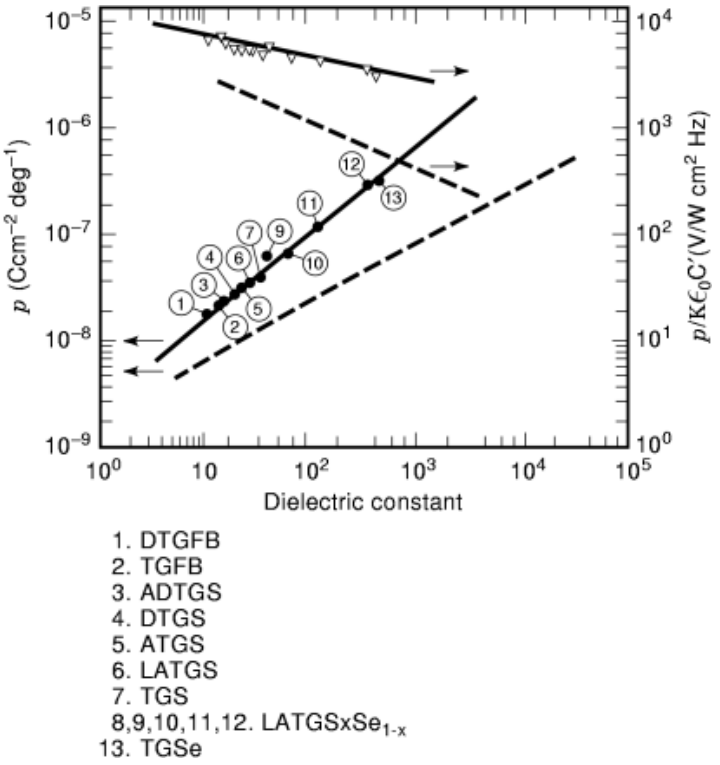

Fig. 4. Pyroelectric coefficients and pyroelectric figure of merit $p/\varepsilon_0 \kappa C'$ versus dielectric constant for various proper ferroelectric materials. Solid lines and broken lines represent the TGS family and the displacive and order-disorder ferroelectrics, respectively, ($C' = \rho C_P$).

In the second category measurements of polarization or charge can be estimated either by the integrating pyroelectric current while continuously heating the sample or recording the hysteresis loop at various temperatures by the Sawyer–Tower technique. The charge release (in either of the two cases) at a discrete temperature is determined, and the pyroelectric coefficient is obtained by graphical methods or differentiation.

BIBLIOGRAPHY

1. A. S. Bhalla, L. E. Cross, Primary and secondary pyroelectricity in proper and improper, *Ferroelectrics*, **38**: 935, 1981.
2. A. S. Bhalla, C. S. Fang, L. E. Cross, Pyroelectric properties of the alanine and arsenic doped triglycine sulphate single crystals, *Appl. Phys. Lett.*, **43**: 932, 1983.
3. J. C. Burfoot, G. W. Taylor, Polar Dielectrics and Their Applications, London: Macmillan, 1979.
4. R. L. Byer, C. B. Roundy, Pyroelectric coefficient direct measurement technique and application to a nanosecond-response-time detector, *Ferroelectrics*, **3**: 333, 1972.
5. A. G. Chynoweth, Dynamic method for measuring the pyroelectric effect with special reference to barium titanate, *Appl. Phys.*, **27**: 78, 1956.
6. Landau-Börnstein, New Series, *Ferro- and Antiferroelectric Materials, Numerical Data and Functional Relationships in Science and Technology*, Vol. **III/3**, 1973, Vol. **III/5**, 1975; Vol. **III/11**, 1978; Vol. **III/18**, 1984; Vol. **III/29**, 1994; H. Hellwege and K. A. Hellwege (eds.), New York: Springer-Verlag.

7. S. B. Lang, Ferroelectrics and related phenomena, in I. Lefkowitz and G. W. Taylor (eds.), Vol. 2, *Source Book of Pyroelectricity*, New York: Gordon & Breach Science, Publishers, 1974.
8. M. E. Lines, A. M. Glass, *Principles and Applications of Ferroelectrics and Related Materials*, Oxford, UK: Oxford University Press, 1977.
9. S. T. Liu, J. D. Zook, D. Long, Relations between pyroelectric and ferroelectric parameters, *Ferroelectrics*, **9**: 39, 1975.
10. J. F. Nye, *Physical Properties of Crystals*, London: Oxford Univ. Press, 1957.
11. L. B. Schein, P. J. Cressman, L. E. Cross, Electrostatic measurements of tertiary pyroelectricity in partially clamped lithium niobate (LiNbO3), *Ferroelectrics*, **22**: 945, 1979.
12. R. W. Whatmore, Pyroelectric devices and materials, *Rep. Prog. Phys.*, **49**: 1335, 1986.
13. Y. Xu, *Ferroelectric Materials and Their Applications*, New York: North-Holland, 1991.

A. S. BHALLA
R. GUO
Pennsylvania State University